CL-171139 Received: December 5, 2017 | Accepted: December 26, 2017 | Web Released: January 12, 2018

# Effect of Channel Geometry on Ionic Current Signal of a Bridge Circuit Based Microfluidic Channel

Hirotoshi Yasaki,*[1,2] Takao Yasui,[1,2,3] Takeshi Yanagida,[4,5] Noritada Kaji,[1,2,3] Masaki Kanai,[4] Kazuki Nagashima,[4] Tomoji Kawai,[5] and Yoshinobu Baba*[1,2,6]

[1]*Department of Biomolecular Engineering, Graduate School of Engineering, Nagoya University, Furo-cho, Chikusa-ku, Nagoya, Aichi 464-8603, Japan*

[2]*ImPACT Research Center for Advanced Nanobiodevices, Nagoya University, Furo-cho, Chikusa-ku, Nagoya, Aichi 464-8603, Japan*

[3]*Japan Science and Technology Agency (JST), PRESTO, 4-1-8 Honcho, Kawaguchi, Saitama 332-0012, Japan*

[4]*Laboratory of Integrated Nanostructure Materials Institute of Materials Chemistry and Engineering, Kyushu University, 6-1 Kasuga-koen, Kasuga, Fukuoka 816-8580, Japan*

[5]*Institute of Scientific and Industrial Research, Osaka University, Mihogaoka, Ibaraki, Osaka 567-0047, Japan*

[6]*Health Research Institute, National Institute of Advanced Industrial Science and Technology (AIST), Takamatsu, Kagawa 761-0395, Japan*

E-mail: yasaki.hirotoshi@e.mbox.nagoya-u.ac.jp (H. Yasaki), babaymtt@chembio.nagoya-u.ac.jp (Y. Baba)

Bridge circuit based ionic current sensing in a microfluidic channel has attracted attention as a highly sensitive analytical method for bio-related molecules and particles. However, channel geometry which greatly influences the detected ionic current has not been investigated. Here, we investigate experimentally and theoretically the effect of differences in the microfluidic channel geometry on shapes and amplitude of signals in ionic current sensing. Our results clarify the geometrical effect of the channel in the bridge circuit based ionic current sensing method.

**Keywords:** Nanopore and micropore | Ionic current sensing | Microfluidic bridge circuit

Ionic current sensing methods with a nano- to microscale channel shaped sensing area offer promising ways to detect DNA molecules,[1–6] RNA molecules,[7,8] proteins,[9] viruses,[10–12] and bacterial cells.[13] The detection mechanism of these methods is based on the electrical resistance change of a sensing area filled with conductive solution that responds to the excluded volume caused by the translocation of sample molecules and particles when applying electrical voltages. Recently, we reported results for high sensitivity sensing using a bridge circuit[14] that exceeded the limit of conventional ionic current sensing methods. We found that a characteristic current signal, which has not been seen using conventional methods, can be obtained in the bridge circuit based ionic current sensing. However, in that study, we did not investigate channel geometry which greatly influences the measured ionic current. By examining the influence of channel geometry on the current response in detail, we expect that additional high sensitivity design guidelines for the bridge circuit based ionic current sensing method can be clarified together with the generation mechanism of the characteristic current signal. In this paper, we observe the signals when microchannels having various structures are used, and we considered the influence of the channel geometry on signal shapes and amplitudes.

Our proposed ionic current sensing was performed using a microfluidic bridge circuit which consists of a microfluidic sensing chip and electric circuits (Figure 1a). The microfluidic bridge circuit, which we had developed previously,[14] is connected to a circuit for balancing potential (balance circuit, black lines) and a circuit for sample flow (sample circuit, red lines) via bridge lines (blue lines) that include an Ampere meter (Figure 1b). In the microfluidic sensing chip, channels for sample flow and bridge lines are connected to the sensing area. A voltage is applied and the current is sensed using silver electrodes (FTVS-408, Oyaide), which are connected to reservoirs of the microfluidic sensing chip. Current flowing through the bridge lines is monitored by the Ampere meter. When there are no particles in the microfluidic sensing chip, the circuit is adjusted to get a balanced state in which no current flows to the Ampere meter, and therefore, the background current baseline becomes about 0 A. As sample particles pass through the sensing area, the potential difference at both ends of the sensing area

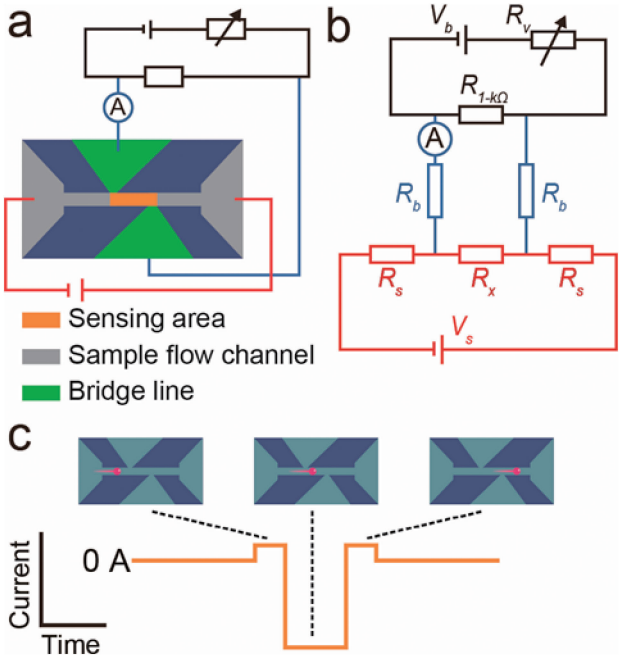


**Figure 1.** Schematic illustrations of bridge circuit based ionic current sensing method and its signal shapes. (a) Schematic illustration of bridge circuit based ionic current sensing method. (b) Diagram of bridge circuit. (c) Signal shapes obtained by the bridge circuit based ionic current sensing method.


© 2018 The Chemical Society of Japan

increases and the balance is lost; as a result, current flows to the Ampere meter and it is detected as a signal. Regardless of sample size, translocation of the sample forms two hills and one valley in the current signal (Figures 1c and S1).[14,15] Amplitude of the valley in the current signal is proportional to sample particle volume, and can be calculated by eq 1.[14]

$$I_{\text{valley}} = (V_s \times \Delta R_x)/[(2R_b + R_x) \times (2R_s + R_x)] \quad (1)$$

Here, $I_{\text{valley}}$ is amplitude of the valley in the current signal, $\Delta R_x$ is resistance change of the sensing area by sample introduction, $V_s$ is applied voltage, $R_b$ is resistance of each bridge line, $R_s$ is resistance of each sample flow channel, and $R_x$ is resistance of the sensing area. This equation holds when $R_{1\text{-}k\Omega}$ is sufficiently small compared with $R_x$ and $R_b$.

Using photolithography techniques, we fabricated microchannels on a polydimethylsiloxane (PDMS) plate (SILPOT 184 Dow Corning, Toray Co., Ltd.). We fabricated the microfluidic sensing chip by bonding a cover glass and the PDMS plate with the microchannels after plasma treatment. We filled 5 × TBE buffer solution (0.45 M Tris, 0.45 M boric acid, 0.01 M EDTA) into the microchannels. Width and height of the sensing area were 4 and 7.5 µm, respectively. Length of the sensing area was varied from 15 to 100 µm by changing the distance between bridge lines. Width of the sample flow channels was varied from 4 to 25 µm.

We used polystyrene microspheres (Fluoresbrite Calibration Grade Microspheres, YG, Polysciences, Inc.) of 0.75, 1.00, 1.10, 1.75, 2.08, and 3.10-µm diameters as sample particles. We diluted each purchased sample solution to $2 \times 10^6$ particles $mL^{-1}$ using distilled water.

Experimental operations have been optimized in our past report,[14] and sample particles are introduced into the sensing area by applying voltage to the microfluidic sensing chip (Figure S2). A voltage of 53 V was applied to the microfluidic sensing chip. The solution containing the sample particles was dropped into the inlet, and the sample particles were introduced into the sensing area from the cathode to the anode by electrophoresis. We recorded the current signals obtained by changing the potential due to passage of the sample particles through the sample flow channels and sensing area. For optical observation of sample passage in the sensing area, a fluorescence microscope (Eclipse Ti, Nikon Corp.) was used which was equipped with a lens of 20× (0.45NA, Nikon Corp.) and a mercury lamp (USH-102D, Ushio Inc.) The microfluidic sensing chip was placed on the microscope stage.

To observe the effect of channel geometry on signal shapes, we changed the distance between bridge lines. When the distance between bridge lines was shortened, the amplitude of the hills and the valley in the current signal decreased and increased, respectively (Figure 2a). According to the principle of the electric resistance calculation, a longer channel length increases the electric resistance. As the distance between bridge lines is narrowed, the length of the sensing area and sample flow channel are decreased and increased, respectively. As a result, the resistance of the sensing area ($R_x$) decreases and the resistance of the sample flow channel ($R_s$) increases. Based on the theoretical equation for amplitude of the valley in the current signal (eq 1), the denominator decreases and the numerator does not change; as a result, the amplitude of the valley in the current signal increases. These expectations were consistent with our

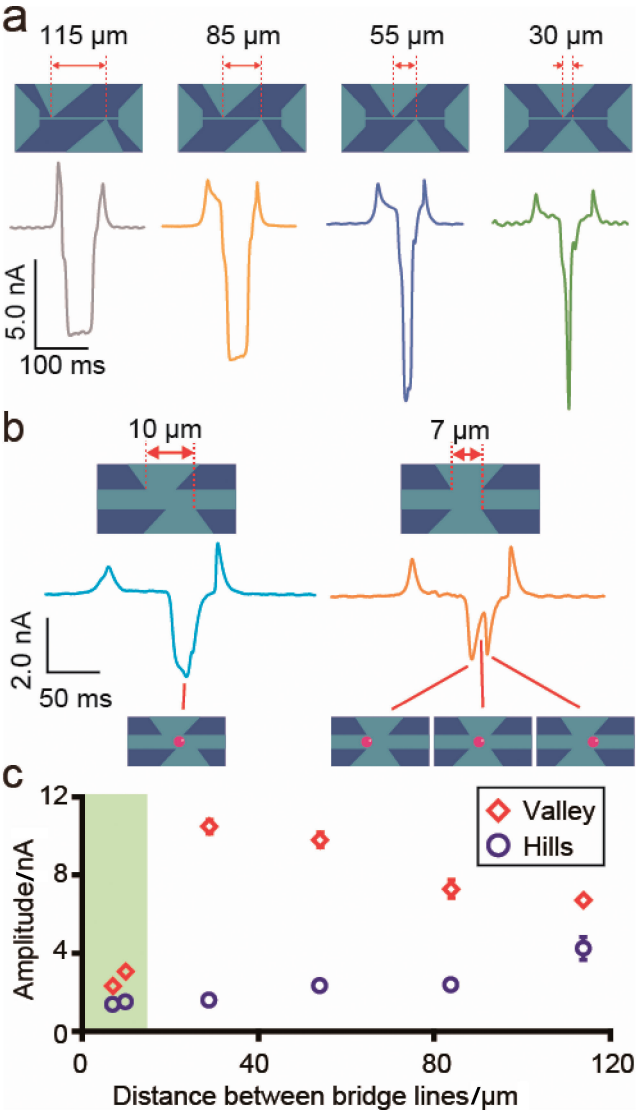


**Figure 2.** Effect of distance between bridge lines on amplitude and shape of the valley and hills in the current signals. (a) Detected signals of a 3.10-µm diameter polystyrene particle obtained by the microfluidic sensing chips shown in the upper. Four distances between bridge lines were used. (b) Signal shapes in the microfluidic sensing chips with partially or completely overlapped bridge lines. Upper illustrations are the microfluidic sensing chips with 2 distances between the overlapped bridge lines. Lower graphs show signal shapes of a 3.10-µm diameter polystyrene particle in the microfluidic sensing chips with overlapped bridge lines. Simultaneous electrical and optical measurements correlated sample particle positions and signal shapes. (c) Comparison of amplitudes of the valley and hills in the current signals at various distances between bridge lines. Green area denotes overlap of bridge lines. Error bars show the standard deviation for a series of measurements (N = 200).

experimental results. Therefore, it became clear that the bridge lines needed to be closer to increase the amplitude of the valley in the current signal.

When we made the distance between the bridge lines too narrow and the positions overlapped, the amplitude of the valley


© 2018 The Chemical Society of Japan

in the current signal decreased and the valley became a double valley (Figure 2b). We carried out a fluorescence observation simultaneously with ionic current sensing,[15] and we examined specific signals based on sample positions and signal shapes. The reason for decreasing amplitude of the valley in the current signal by the partial overlapped bridge lines positions was that the narrow space in the sensing area disappeared and the resistance increased because the sample translocation weakened. On the other hand, the reason for occurrence of the double valley in the current signal by the completely overlapped bridge line positions was that the 7-μm channel width of the bridge line was larger than the 3.10-μm diameter sample particle and the resistance value was hardly increased when the sample was at the center of the sensing area. Therefore, in order to increase the amplitude of the valley in the current signal, it is important to make the sensing area with bridge lines as close as possible without overlapping (Figure 2c).

When we observed the shape of hills in the current signal, it became clear that the amplitudes of the hills were affected by channel resistance the same as the valley in the current signal. Therefore, in this study, we derived a theoretical equation to calculate current change based on resistance change of a sample flow channel by sample introduction, and compared theoretical and experimental values. Using the principle of the bridge circuit based sensing,[14] we derived the following theoretical equation (eq 2) for estimating the amplitude of hills in the current signal due to resistance change when a sample particle was present in the sample flow channels (Figure S3 and derivation of theoretical equation in Supporting Information).

$$I_{\text{hill}} = (V_s \times R_x \times \Delta R_s)/[(2R_b + R_x) \times (2R_s + R_x)^2] \quad (2)$$

Here, $I_{\text{hill}}$ is amplitude of hills in the current signal and $\Delta R_s$ is resistance change of each sample flow channel by sample introduction. This equation holds when $R_v$ and $R_{1\text{-}k\Omega}$ are sufficiently small compared with $R_x$ and $R_b$. When we decrease the sensing area resistance and increase the sample flow channel resistance by shortening the distance between bridge lines, the denominator decreases slightly and the numerator decreases greatly; as a result, the amplitudes of hills in the current signal decrease. These expectations were consistent with experimental results in Figure 2a. The validity of the tendency expected from the theoretical equations was proved. On the other hand, experimental results did not show symmetry in time change of signal shapes. One of possibilities for this results is that a particle passed before the ionic current sufficiently reflected the sudden change of electric field in the bridge lines when the particle moves in the sample flow channels and the sensing area.

For validation of theoretical values, the theoretical value for 3.10-μm diameter polystyrene particle detection was compared with 100 overlaid signals of the experimental results (Figure 3). Average value of amplitudes of hills was used for validation because there was no systematic error in the amplitude difference of front and rear hills (Figure S4). In the detection of 3.10-μm diameter polystyrene particles in the sensing area (7.5 μm height × 4.0 μm width × 70 μm length), resistance of the sample circuit ($2R_S + R_x$) was 21.6 MΩ. The sum of resistances of the bridge lines and the sensing area ($2R_b + R_x$) was 11.7 MΩ. Applied voltage ($V_s$) was 53 V. Based on the excluded volume by introduction of the 3.10-μm diameter polystyrene particles, resistance change of the sensing area ($\Delta R_x$) and sample flow

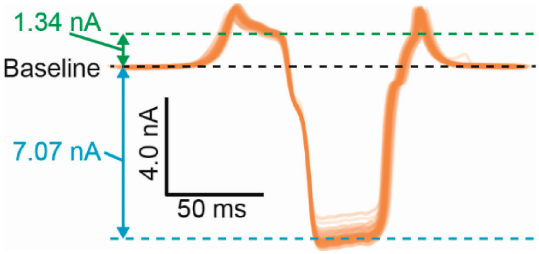


**Figure 3.** Validation of theoretical equation. Orange curves are the overlay of 100 signals of a 3.10-μm diameter polystyrene particle in the bridge circuit based ionic current sensing method. The black dashed line is the base line of ionic current sensing. The blue dashed line is calculated amplitude of the valley in the current signals based on eq 1. The green dashed line is calculated amplitude of hills in the current signals based on eq 2.

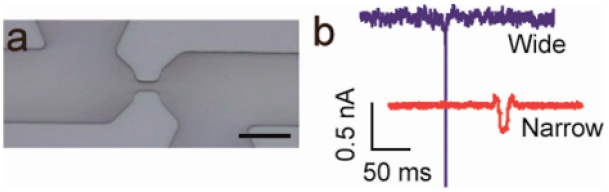


**Figure 4.** Effect of width of a sample flow channels on existence of hills in the current signal. (a) A photo of the microfluidic sensing chip with the wide sample flow channel; scale bar, 15 μm. (b) Comparison of signal shapes of a 1.00-μm diameter polystyrene particle in the microfluidic sensing chip with the wide (blue line) and narrow (red line) sample flow channels.

channel ($\Delta R_s$), which had 7.5 μm height and 4.0 μm width, was 33.7 kΩ for each. Using eqs 1 and 2, we could calculate $I_{\text{valley}}$ and $I_{\text{hill}}$ as 7.07 and 1.34 nA, respectively. Because the calculated amplitudes of hills and the valley in the current signal were almost comparable to the experimental values of the 100 overlaid signals, it became clear that the change of the resistance value by eliminating the conductive solution in the sample flow channel and the sensing area caused hills and the valley in the current signal, respectively. Since $\Delta R_s$ is determined by the ratio of the sample particle volume to the sample flow channel volume, the amplitude of hills in the current signal can be changed easily by changing the volume ratio of sample particles to sample flow channel (Figure 2c).

Based on the theoretical equation, for a larger sample flow channel hills would disappear in the current signal and amplitude of the valley would increase. When we expanded the width of the sample flow channel to 25 μm, only the valley in the current signal was obtained (Figure 4). Using the theoretical equation for hills in the current signal (eq 2), we calculated the amplitude of hills in the current signal at this time to be 2.4 pA, which was smaller than the baseline noise value of 70 pA. For this reason, only the valley in the current signal was observed. Increasing the width of the sample flow channel also led to an increase in the amplitude of the valley in the current signal; as a result, samples could be detected with higher sensitivity compared with sensitivity of other structures which have narrow sample flow channels.


© 2018 The Chemical Society of Japan

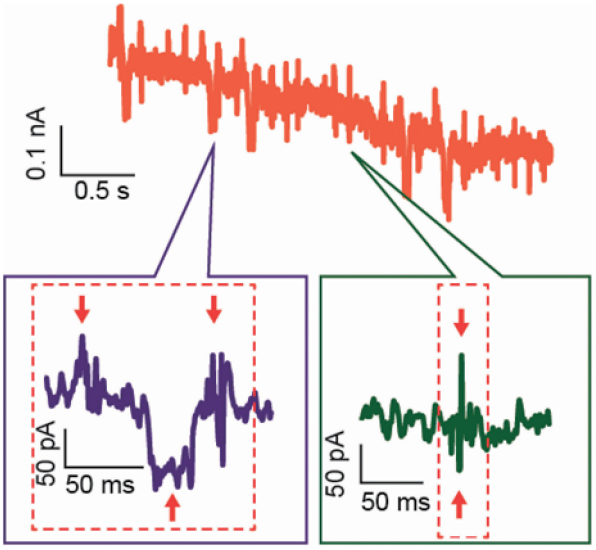


**Figure 5.** Comparison between the current signal and the spike noise. In the current sensing (orange line), the current signal (blue line) had two hills and one valley (marked by red arrows). On the other hand, the spike noise (green line) did not have two hills and one valley at the same time. Based on the difference of signal shapes, signals and noise could be discriminated.

In the series circuit based ionic current sensing method, a resistance increase before or after the sensing area changes amplitude and shape of the valley in the current signal.[16] Therefore, the bridge circuit based ionic current sensing method detects the opposite direction current change. Even when spike noise occurred during measurements, the current signal including two hills and one valley could be easily discriminated because spike noise did not have hills and the valley at the same time (Figure 5).

In conclusion, in the bridge circuit based ionic current sensing method, the amplitudes of hills and the valley in the current signal were determined by the ratio of the sample volume to the sample flow channel volume and the sample volume to the sensing area volume, respectively. The theoretical equation for predicting hills in the current signal when the sample passes through the sample flow channels was derived and the amplitudes were calculated. By changing the geometry of the sensing area and the sample flow channels, their geometrical effect on signal amplitudes and shapes was obtained. Hills in the current signal can be arbitrarily detected by changing the channel structure. By widening the sample flow channels so as not to detect hills in the current signal, the amplitude of the valley in the current signals could be increased. On the other hand, by narrowing the sample flow channels to detect hills in the current signal, the clarity of the current signal could be increased. These findings will allow researchers to design microfluidic channels for obtaining optimal signal shapes depending on the experimental purpose.

This research was supported by Grant-in-Aid for JSPS Research Fellow No. 15J03490, PREST (Nos. JPMJPR151B, JPMJPR16F4), JST, the JSPS Grant-in-Aid for Young Scientists (A) No. 17H04803, the ImPACT Program of the Council for Science, Technology and Innovation (Cabinet Office, Government of Japan), and the JSPS Grant-in-Aid for Scientific Research (A) No. 16H02091.

Supporting Information is available at http://dx.doi.org/10.1246/cl.171139.

## References

1 J. Li, M. Gershow, D. Stein, E. Brandin, J. A. Golovchenko, *Nat. Mater.* **2003**, *2*, 611.
2 U. F. Keyser, B. N. Koeleman, S. van Dorp, D. Krapf, R. M. M. Smeets, S. G. Lemay, N. H. Dekker, C. Dekker, *Nat. Phys.* **2006**, *2*, 473.
3 J. Clarke, H.-C. Wu, L. Jayasinghe, A. Patel, S. Reid, H. Bayley, *Nat. Nanotechnol.* **2009**, *4*, 265.
4 L. D. Menard, C. E. Mair, M. E. Woodson, J. P. Alarie, J. M. Ramsey, *ACS Nano* **2012**, *6*, 9087.
5 A. T. Carlsen, O. K. Zahid, J. A. Ruzicka, E. W. Taylor, A. R. Hall, *Nano Lett.* **2014**, *14*, 5488.
6 C. Plesa, J. W. Ruitenberg, M. J. Witteveen, C. Dekker, *Nano Lett.* **2015**, *15*, 3153.
7 M. Ayub, S. W. Hardwick, B. F. Luisi, H. Bayley, *Nano Lett.* **2013**, *13*, 6144.
8 C. Shasha, R. Y. Henley, D. H. Stoloff, K. D. Rynearson, T. Hermann, M. Wanunu, *ACS Nano* **2014**, *8*, 6425.
9 J. Nivala, D. B. Marks, M. Akeson, *Nat. Biotechnol.* **2013**, *31*, 247.
10 R. W. DeBlois, R. K. Wesley, *J. Virol.* **1977**, *23*, 227.
11 K. Zhou, L. Li, Z. Tan, A. Zlotnick, S. C. Jacobson, *J. Am. Chem. Soc.* **2011**, *133*, 1618.
12 Z. D. Harms, D. G. Haywood, A. R. Kneller, L. Selzer, A. Zlotnick, S. C. Jacobson, *Anal. Chem.* **2015**, *87*, 699.
13 G. Goyal, R. Mulero, J. Ali, A. Darvish, M. J. Kim, *Electrophoresis* **2015**, *36*, 1164.
14 H. Yasaki, T. Yasui, T. Yanagida, N. Kaji, M. Kanai, K. Nagashima, T. Kawai, Y. Baba, *J. Am. Chem. Soc.* **2017**, *139*, 14137.
15 H. Yasaki, T. Yasui, S. Rahong, T. Yanagida, N. Kaji, M. Kanai, K. Nagashima, T. Kawai, Y. Baba, *Proc. μTAS2014* **2014**, *1*, 2161.
16 N. Yukimoto, M. Tsutsui, Y. He, H. Shintaku, S. Tanaka, S. Kawano, T. Kawai, M. Taniguchi, *Sci. Rep.* **2013**, *3*, 1855.


© 2018 The Chemical Society of Japan 